


Short Communication

Deletion of Galectin-3 attenuates acute pancreatitis in mice by affecting activation of innate inflammatory cells

Bojan Stojanovic^{1,2}, Ivan Jovanovic¹, Bojana S. Stojanovic^{1,3},
Milica Dimitrijevic Stojanovic¹, Nevena Gajovic¹, Gordana Radosavljevic¹,
Jelena Pantic¹, Nebojsa Arsenijevic¹ and Miodrag L. Lukic¹ 

¹ Center for Molecular Medicine and Stem Cell Research, Faculty of Medical Sciences, University of Kragujevac, Kragujevac, Serbia

² Department of Surgery, Faculty of Medical Sciences, University of Kragujevac, Kragujevac, Serbia

³ Department of Pathophysiology, Faculty of Medical Sciences, University of Kragujevac, Kragujevac, Serbia

Acute pancreatitis is characterized by autodigestion of pancreatic cells followed by acute inflammation leading to pathology and death. In experimental acute pancreatitis, pancreatic acinar cells and infiltrating macrophages express Galectin-3 but its role in pathology of this disease is unknown. Therefore, we studied its role using Galectin-3 deficient mice. Deletion of Galectin-3 prolonged the survival of mice, led to attenuation of histopathology, and decreased infiltration of mononuclear cells and neutrophils that express TLR-4, in particular, pro-inflammatory N1 neutrophils. Galectin-3 and TLR-4 are also colocalized on infiltrating cells. Lack of Galectin-3 reduced expression of pro-inflammatory TNF- α and IL-1 β in F4/80⁺CD11c⁻ and CD11c⁺F4/80⁻ cells. Thus, deletion of Galectin-3 ameliorates acute pancreatitis by attenuating early influx of neutrophils and inflammatory mononuclear cells of innate immunity. These findings provide the basis to consider Galectin-3 as a therapeutic target in acute pancreatitis.

Keywords: acute pancreatitis · Galectin-3 · N1 neutrophils · TLR4

Introduction

Acute pancreatitis (AP) is an acute inflammation of pancreatic tissue initiated by intra-acinar activation of proteolytic enzymes in a cathepsin-B-dependent and calcium-dependent manner [1]. Activated proteolytic enzymes cause destruction of acinar cells and release of inflammatory cytokines [2]. Injured acinar cells also release intracellular content into the extracellular space that serves as damage-associated molecular patterns attracting inflammatory cells that can cause further damage of pancreas [2].

Galectin-3 (Gal-3) is a member of galectins family with a unique chimeric structure and plays important pro-inflammatory role in inflammatory and autoimmune diseases [3]. Under physiological conditions in mice, only duct epithelium cells of pancreas express Gal-3 [4]. After the induction of pancreatitis, acinar cells start to express Gal-3, and there is an increased expression of Gal-3 in infiltrating cells [4].

Here, we demonstrated that Gal-3 deficient mice survived longer after bile–pancreatic duct (BPD) ligation as a model of the severe and lethal form of AP. In addition, we showed that deletion of Gal-3 contributes to a significant attenuation of AP accompanied by decreased influx of neutrophils and mononuclear cells into the pancreas, and decreased accumulation of pro-inflammatory innate immune cells.

Correspondence: Prof. Miodrag L. Lukic
e-mail: miodrag.lukic@medf.kg.ac.rs

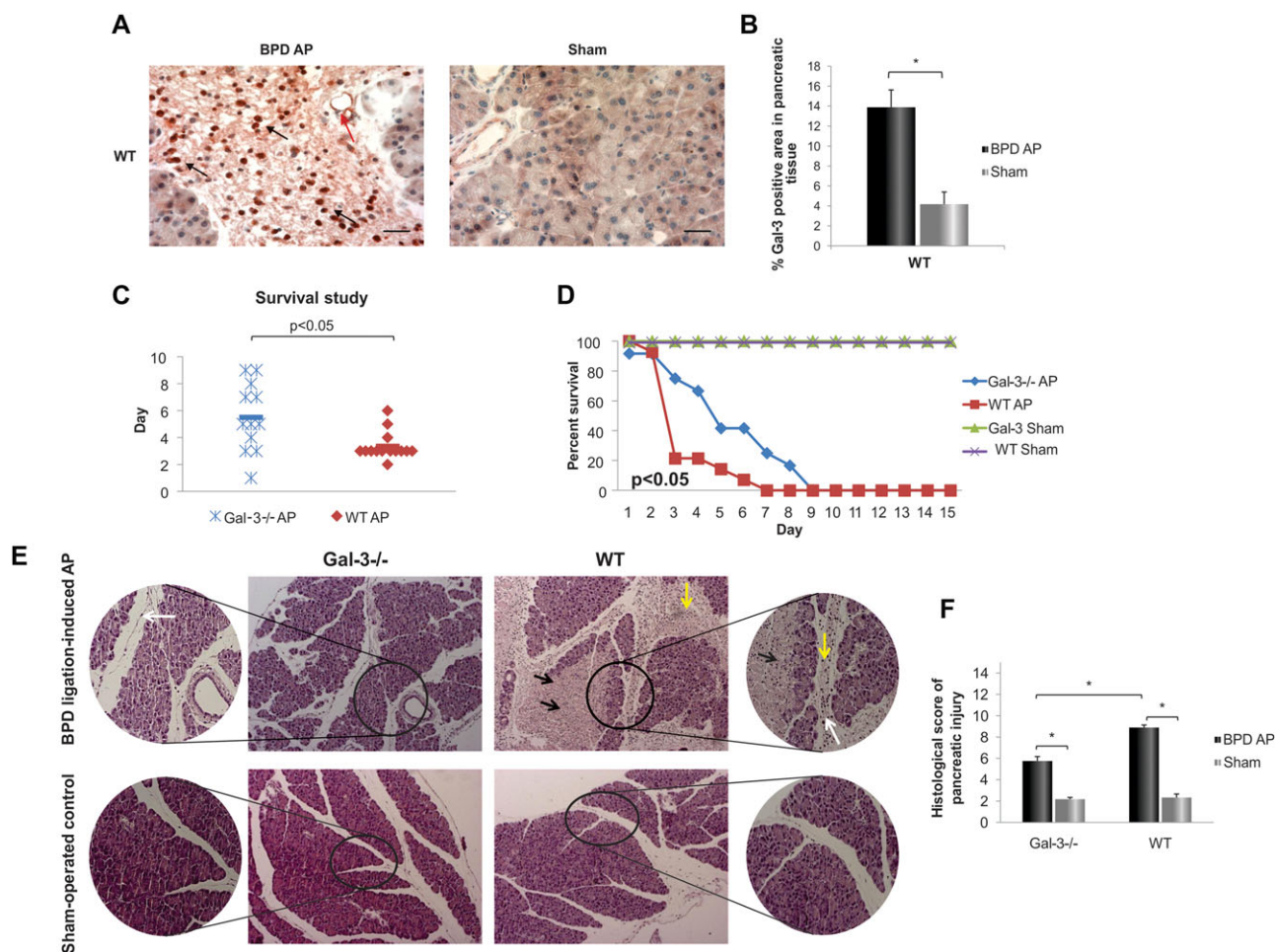


Figure 1. Target disruption of Gal-3 prolongs survival of mice with acute pancreatitis and suppresses disease induced by BPD ligation. (A) Immunohistochemical staining showing expression of Gal-3 in duct cells (red arrow) and infiltrating cells (black arrows) in the pancreas samples obtained from diseased (left panel) and control animals (right panel). Scale bar: 100 μ m. Images are representative of two independent experiments with 10 mice per group in each experiment. (B) Percentage of expression of Gal-3 in pancreata of diseased and control mice. (C) Scatter plot of mortality in mice with BPD ligation-induced AP. (D) Kaplan–Meier curve presents survival rate in BPD ligation model of AP. Data shown are pooled from two independent experiments with seven mice per group per experiment. (E) Photomicrographs of representative H&E-stained mouse pancreas 72 h after BPD ligation-induced AP. Massive pancreatic necrosis (black arrows), massive inflammatory cell infiltration (yellow arrows) and intralobular edema (white arrows) were observed in WT mice in comparison, to a lesser extent of pancreatic damage observed in Gal-3^{-/-} mice characterized only with intralobular and inter-acinar edema (white arrows). Photomicrographs of representative H&E-stained mouse pancreas from sham-operated controls that were without signs of pancreatic injury. Scale bar: 200 μ m. Images are representative of two independent experiments (12 mice per group in each experiment). (F) Total histological score of AP, * $p < 0.05$, Mann–Whitney U-test.

Taken together, our data demonstrate that Gal-3 plays an important pro-inflammatory role and may be a potential therapeutic target in pancreatitis.

Results and discussion

Galectin-3 deletion prolongs survival of mice with acute pancreatitis and attenuates tissue damage

We found intracytoplasmic and intranuclear increased expression of Gal-3 in the infiltrating leukocytes within 72 h after AP induction by BPD ligation, indicating its involvement in pathology

(Fig. 1A and B). This correlates with previous reported enhanced expression of Gal-3 in experimental pancreatitis [4].

In accordance with previous findings [5], we showed that “wild-type” (WT) mice with a lethal form of AP-induced by BPD ligation showed 100% mortality within 5 days, with a median mortality at day 3 (Fig. 1C). However, Galectin-3 deficient (Gal-3^{-/-}) mice with a lethal form of AP-induced by BPD ligation showed 100% mortality within 9 days, with median mortality at day 5 (Fig. 1C). Thus, Gal-3^{-/-} mice with AP survived significantly longer in comparison to WT mice with AP (Fig. 1C). Also, Kaplan–Meier curves revealed significant difference in survival rate between WT and Gal-3^{-/-} mice with AP (Fig. 1D). As expected, both sham-operated controls had 100% survival at 15 days (Fig. 1D). It appears that longer survival of Gal-3^{-/-} mice is

related to milder inflammatory response as illustrated in Figure 1E and G. Specifically, 72 h after BPD ligation, histological analysis of H&E-stained pancreatic section revealed that WT mice with AP showed significantly more severe edema, leukocyte infiltration, and widespread areas of necrosis and vacuolization of pancreatic parenchyma that were not seen in Gal-3^{-/-} mice (Fig. 1E). Total acute pancreatitis histological score was markedly lower in Gal-3^{-/-} mice with AP compared with WT mice (Fig. 1F). Our results are in line with those of Pan et al. [6] who showed that treatment with lactose, an inhibitor of galectins, alleviated the severity of experimental AP.

Gal-3 deficiency decreases early influx of TLR-4+ innate inflammatory cells in AP

Seventy-two hours after BPD ligation, total number of infiltrating leukocytes in pancreatic tissue was significantly higher in WT mice with AP compared with Gal-3^{-/-} mice with AP (Fig. 2A). After induction of AP, there was significant influx of neutrophils into the pancreas (Fig. 2B). The total number of these cells was significantly higher in pancreata of WT mice than Gal-3^{-/-} mice (Fig. 2B), although the difference in the percentage of neutrophils did not reach statistical significance (Fig. 2C). The percentage of F4/80⁺CD11c⁻ cells and total number of these cells were significantly higher in WT mice compared to Gal-3^{-/-} mice (Fig. 2D and E). Immunohistochemical analysis confirmed increased infiltration of Ly-6G/Ly-6C⁺ cells (Fig. 2F) and F4/80⁺ cells (Fig. 2H), with significantly increased percentage of Ly-6G/Ly-6C⁺ cells (Fig. 2G) and F4/80⁺ cells (Fig. 2I) in pancreata of diseased WT mice compared to Gal-3 deficient mice. It is well known that Gal-3 promotes leukocyte recruitment and may act as an adhesion molecule when it is present in inflammatory exudates [7].

Also, Gal-3^{-/-} mice with AP exhibited significantly lower percentage (Fig. 2K) and total number of TLR-4-expressing neutrophils in comparison to WT mice (Fig. 2J). Similarly, level of TLR-4 expression was significantly decreased on individual neutrophils derived from diseased Gal-3^{-/-} mice in comparison to diseased WT mice (Fig. 2L). In line with these findings, we also performed immunofluorescent double staining with anti-TLR-4 and anti-F4/80 antibodies, as well as anti-Ly-6G/Ly-6C antibody. As expected, WT mice with AP had increased infiltration of Ly-6G/Ly-6C⁺ neutrophils that express TLR-4 (Fig. 2M) and F4/80⁺ cells that express TLR-4 (Fig. 2O). Quantitative immunofluorescence of the pancreatic tissue revealed significantly greater number of TLR-4-positive neutrophils (Fig. 2N) and TLR-4-positive F4/80 cells (Fig. 2P) in diseased WT animals compared to Gal-3^{-/-} animals. The analysis summarized in Figure 2Q shows colocalization of TLR-4 and Gal-3 on the same leukocytes in infiltrate. Consistent with these findings, it is shown that Gal-3 is ligand for TLR-4 in experimental neuroinflammation [8, 9]. Further, target deletion of TLR-4 gene ameliorates experimental AP by significantly reduced influx of neutrophil and tissue damage in severe AP [10].

Gal-3 deletion attenuates influx of N1 neutrophils and pro-inflammatory accessory cells

Neutrophils, key players in acute inflammation, play crucial role in a course of AP and infiltrate the pancreas within first hours after induction of experimental model of AP [11]. After the induction of AP, Gal-3^{-/-} mice had significantly lower number of neutrophils compared to WT mice (Fig. 2B). In tumor model, Fridlender et al. [12] described two types of neutrophils: N1 neutrophils and N2 neutrophils. N1 neutrophils secrete higher level of pro-inflammatory cytokines, such as TNF- α and IL-1 β , oxygen radicals, and are more potent in activating cytotoxic T lymphocytes. At the molecular level, N1 neutrophils express higher levels of FasL molecule. We found that the total number of FasL-expressing neutrophils was significantly higher in WT mice compared to Gal-3^{-/-} mice (Fig. 3A). Furthermore, we found significantly higher expression of FasL per neutrophils isolated from pancreata of WT mice compared to Gal-3^{-/-} mice with AP (Fig. 3C). Importantly, pancreata of WT mice had significantly higher percentage and total number of IL-1 β -producing neutrophils (Fig. 3D and E).

As shown previously (Fig. 2D), the total number of F4/80⁺CD11c⁻ cells was significantly lower in pancreata of Gal-3^{-/-} mice. Intracellular staining shown significantly lower the total number of these cells that produce TNF- α in Gal-3^{-/-} mice with AP (Fig. 3F). Also, the pancreata of Gal-3^{-/-} mice had lower total number of F4/80⁺CD11c⁻ cells that produce IL-1 β compared to WT mice with AP (Fig. 3H). Intracellular staining of CD11c⁺F4/80⁻ cells revealed that WT mice with AP had significantly increased total number of TNF- α -producing CD11c⁺F4/80⁻ cells (Fig. 3J). Furthermore, AP induction markedly decreased total number of IL-1 β -producing CD11c⁺F4/80⁻ cells in Gal-3^{-/-} mice in comparison to WT mice (Fig. 3L). Our results were also in accordance with those of Yip et al. [9] that have shown in the model of traumatic injury neutralizing anti-Gal-3 antibody decreased expression of IL-1 β and TNF- α .

Concluding remarks

In summing up, deletion of Gal-3 expressed in inflammatory cells ameliorates AP by attenuating inflammatory response after disease induction. This is evident by lower infiltration of innate immune cells. This is also supported by decreased production of pro-inflammatory TNF- α and IL-1 β .

Materials and methods

Animals

We used 6–8 weeks old Gal-3^{-/-} mice on C57BL/6 background and WT C57BL/6 mice in all experiments. Targeted deletion of Gal-3 gene was done in C57BL/6 embryonic stem cells by Hsu et al. as previously described [13]. Breeding pairs of Gal-3^{-/-}

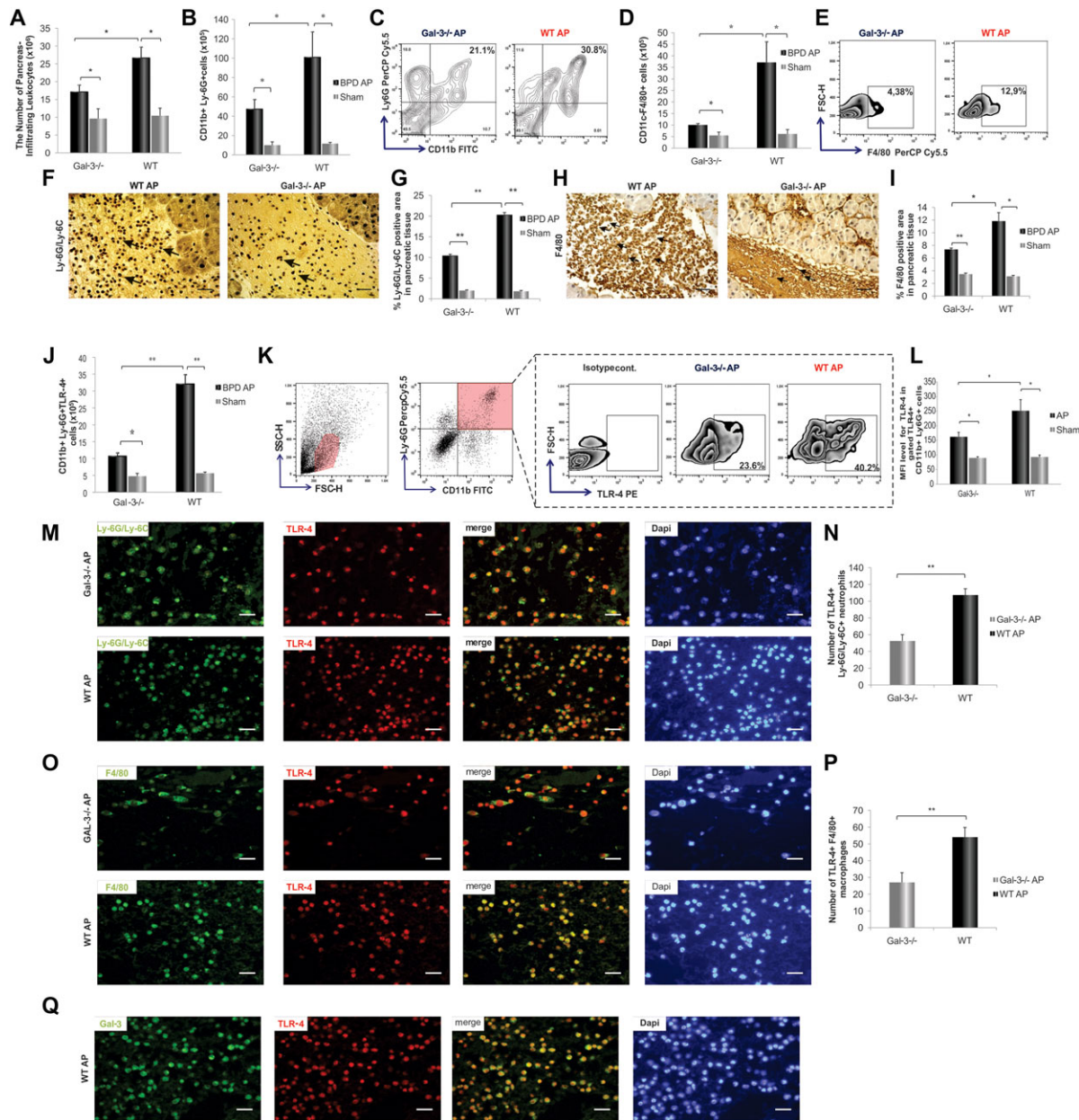


Figure 2. The number of infiltrating cells is lower in the pancreas of Gal-3^{-/-} mice with BPD ligation-induced acute pancreatitis. (A) The total number of pancreas-infiltrating leukocytes was determined by flow cytometry. The total number and representative flow cytometry plots illustrating percentages of neutrophils (B, C) and macrophages (D, E). The total number was calculated per pancreas. Data are shown as the mean ± SEM of 12 mice per group per experiment and are pooled from two independent experiments. **p* < 0.05; Student's *t*-test. (F) The representative immunohistochemical image of infiltration of Ly-6G/Ly-6C⁺ neutrophils (black arrows). Scale bar: 100 μm. Images are representative of two independent experiments (12 mice per group in each experiment). (G) Immunohistochemical analyses of the amount of Ly-6G/Ly-6C-positive areas were performed on pancreatic tissue sections. **p* < 0.05; Student's *t*-test. (H) Representative immunohistochemical image of infiltration of F4/80⁺ cells (black arrows). Scale bar: 100 μm. Images are representative of two independent experiments (12 mice per group in each experiment). (I) Quantitative immunohistochemistry of the F4/80-positive area in pancreata. **p* < 0.05; Student's *t*-test. The total number and representative FACS plots illustrating percentages of TLR-4-expressing neutrophils (J and K). Data are shown as mean ± SEM of 12 mice per group per experiment from two independent experiments, **p* < 0.05; ***p* < 0.001; Student's *t*-test. (L) Quantification of mean fluorescence intensity (MFI) level for TLR-4 in gated CD11b⁺ Ly-6G⁺ cells. (M) Double immunofluorescent staining of Ly-6G/Ly-6C (green) and TLR-4 (red) together with DNA staining with DAPI (blue) in pancreata from representative Gal-3^{-/-} (top) and WT mice with AP (bottom). Scale bar: 25 μm. Images are representative of two independent experiments (10 mice per group in each experiment). (N) Number of TLR-4⁺ neutrophils from pancreata 72 h after BPD ligation. Data are shown as the mean ± SEM, **p* < 0.05; ***p* < 0.001; Student's *t*-test. (O) Immunofluorescent double staining using an anti-F4/80 antibody (red) and an anti-TLR-4 antibody (green) together with DNA staining with DAPI (blue) in pancreata from representative Gal-3^{-/-} (top) and WT mice with AP (bottom). Scale bar: 25 μm. Images are representative of two independent experiments (10 mice per group in each experiment). (P) Number of TLR-4⁺ macrophages from pancreata of diseased animals 72 h after BPD ligation. Data are shown as the mean ± SEM, ***p* < 0.001; Student's *t*-test. (Q) Colocalization of Gal-3 and TLR-4 in infiltrating cell in pancreata 72h after induction of AP. Scale bar: 25 μm. Images are representative of two independent experiments (10 mice per group in each experiment).

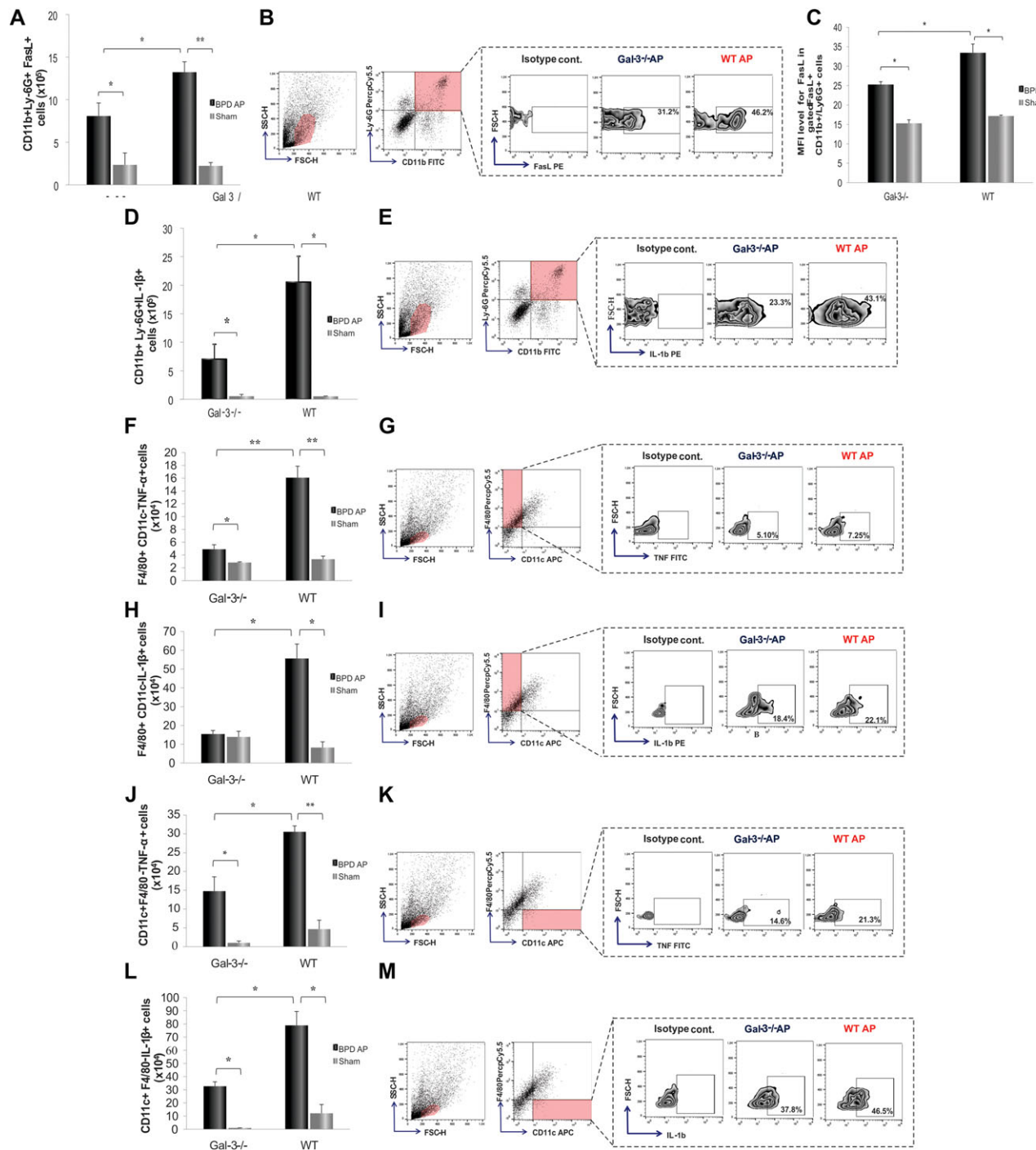


Figure 3. Galectin-3 deletion diminishes pro-inflammatory phenotypes of innate immune cells. The total number and representative flow cytometry plots displaying the frequency of FasL-expressing neutrophils (A, B). (C) Quantification of MFI level for FasL in gated CD11b⁺Ly6G⁺ cells. The total number and representative flow cytometry plots displaying the frequency of IL-1β-producing neutrophils (D, E), TNF-α-producing F4/80⁺CD11c⁻ cells (F, G), IL-1β-producing F4/80⁺CD11c⁻ cells (H, I), TNF-α-producing CD11c⁺F4/80⁻ cells (J, K), and IL-1β-producing CD11c⁺F4/80⁻ cells (L, M), derived from the pancreas. Data are shown as mean ± SEM of 12 mice per group per experiment and are pooled from two independent experiments, **p* < 0.05; ***p* < 0.001, two-tailed unpaired Student's *t*-test.

and WT C57BL/6 mice of the same substrain were housed in a temperature-regulated environment with 12-h light–dark cycle in conventional facilities of the Faculty of Medical Sciences, University of Kragujevac, Serbia. All experiments were approved by the Ethics Board of Faculty of Medical Science and were performed in accordance with relevant guidelines and regulations.

Induction of acute pancreatitis by BPD ligation

Acute pancreatitis was induced by BPD ligation to mimic severe gallstone-induced pancreatitis as described by Samuel et al. [5]. The groups in the experiment were: Gal-3^{-/-} mice with BPD ligation, WT mice with BPD ligation, Gal-3^{-/-} mice with sham operation, and WT mice with sham operation. For survival studies, we observed mice twice daily after BPD ligation. Mice were sacrificed by euthanasia when they showed signs of marked distress and suffering or on day 15 if without clinical signs of disease. For the determination of disease severity and analysis of infiltrating cells, mice were sacrificed 72 h after surgery.

Histopathological and cellular analysis of pancreas

Portions of pancreata from all animal groups were fixed in formalin and embedded in paraffin and 5 mm sections were stained with H&E. Sections were analyzed in a blindly fashion by two observers. The scoring system used as previously suggested.

Pancreatic leukocytes were isolated using collagenase digestion method, as previously described [14]. Flow cytometric analysis was performed as detailed in Cossarizza et al. [15]. The cells were labeled with the following monoclonal antibodies: anti-mouse CD11b, TNF- α , CTLA-4, and F4/80Abs conjugated with fluorescein isothiocyanate (FITC, BD Bioscience, Franklin Lakes, NJ); anti-mouse FasL, and IL-1 β Abs conjugated with PE (BD Bioscience); anti-mouse Ly-6G, CD11c and F4/80 Abs conjugated with peridinin chlorophyll protein (PerCP, BD Biosciences); and anti/mouse and CD11b Abs conjugated with allophycocyanin (APC, BD Bioscience). For intracellular staining, the cells were activated as previously described [16]. Flow cytometric analysis was conducted on a BD Biosciences FACS Calibur and analyzed by using the FlowJo software (Tree Star, Ashland, OR).

Immunohistochemistry of mouse pancreatic samples

Formalin-fixed, paraffin-embedded mouse pancreatic tissue sections were incubated with rabbit anti-mouse F4/80 (ab100790, Abcam, Cambridge, UK) and Gal-3 (ab53082, Abcam), and rat anti-mouse Ly-6G/Ly-6C (RB6-8C5, Novusbio, Littleton, CO, USA). Sections were visualized by rabbit-specific conjugate (ZytoChem Plus HRP Kit; Zytomed, Berlin, Germany), and rat-specific HRP-conjugated antibody (HAF005, R&D Systems, D Systems, Minneapolis, MN) and photomicrographed with a digital camera mounted on the light microscope (Olympus BX51). The

cells stained brown were considered as positive and results are expressed as percent positive staining in the pancreata calculated using Image J software.

Immunofluorescent staining was performed using rabbit anti-mouse F4/80 (1:800), Gal-3 (1:500) antibodies (Abcam), followed by incubation with goat anti-rabbit IgG antibody conjugated with FITC (1:1000; Abcam), then using rat anti-mouse TLR-4 antibody (1:10; R&D Systems), followed by incubation with donkey anti-rat IgG antibody conjugated with PE (1:150, Abcam); and using rat anti-mouse Ly-6G/Ly-6C Antibody (1:500, Novus Biologicals, CO, USA), followed by incubation with donkey anti-rat antibody conjugated with biotin (1:500, Abcam) and goat anti-biotin antibody conjugated with FITC (1:100, Abcam). The sections were mounted with ProLong Gold antifade reagent with DAPI (Invitrogen, Thermo Fisher Scientific, USA). Images were obtained and analyzed using an immunofluorescence microscope (Olympus BX51). Only brightness and contrast were adjusted. Results are presented as a mean count of double-stained cells per field.

Statistical analysis

All data are presented as the mean \pm SEM. The normality of distribution was tested by Kolmogorov–Smirnov test. The two-tailed Student's *t*-test or nonparametric Mann–Whitney rank-sum test were used depending on the normality of distribution. The results were considered significantly different when $p < 0.05$. The data were analyzed using SPSS version 20, statistical package.

Acknowledgements: Funding for this work was provided by grants from the Serbian Ministry of Science and Technological Development (175069, 175071 and 175103), Serbia and from the Faculty of medical sciences, Kragujevac (project JP 06/15), Serbia. The authors thank Professor Dr Irena Tanaskovic for assistance in histopathological assessment, and Aleksandar Ilic and Milena Jurisevic for excellent technical assistance.

Conflict of interest: The authors declare no commercial or financial conflict of interest.

- 1 Talukdar, R., Sareen, A., Zhu, H., Yuan, Z., Dixit, A., Cheema, H., George, J. et al., Release of Cathepsin B in Cytosol Causes Cell Death in Acute Pancreatitis. *Gastroenterology* 2016. 151: 747–758.e745.
- 2 Lankisch, P. G., Apte, M. and Banks, P. A. Acute pancreatitis. *Lancet* 2015. 386: 85–96.
- 3 Radosavljevic G.D., P. J., Jovanovic I., Lukic M.L. and Arsenijevic N. The two faces of galectin-3: roles in various pathological conditions. *Ser. J. Exp. Clin. Res.* 2016. 17: 187–198.

- 4 Gebhardt, A., Ackermann, W., Unver, N. and Elsasser, H. P. Expression of galectin-3 in the rat pancreas during regeneration following hormone-induced pancreatitis. *Cell Tissue Res* 2004. **315**: 321–329.
- 5 Samuel, I., Yuan, Z., Meyerholz, D. K., Twait, E., Williard, D. E. and Kempuraj, D. A novel model of severe gallstone pancreatitis: murine pancreatic duct ligation results in systemic inflammation and substantial mortality. *Pancreatology* 2010. **10**: 536–544.
- 6 Pan, L. L., Deng, Y. Y., Wang, R., Wu, C., Li, J., Niu, W., Yang, Q. et al., Lactose induces phenotypic and functional changes of neutrophils and macrophages to alleviate acute pancreatitis in mice. *Front. Immunol.* 2018. **9**: 751.
- 7 Gittens, B. R., Bodkin, J. V., Nourshargh, S., Perretti, M. and Cooper, D. Galectin-3: a positive regulator of leukocyte recruitment in the inflamed microcirculation. *J. Immunol.* 2017. **198**: 4458–4469.
- 8 Burguillos, M. A., Svensson, M., Schulte, T., Boza-Serrano, A., Garcia-Quintanilla, A., Kavanagh, E., Santiago, M. et al., Microglia-secreted Galectin-3 acts as a Toll-like receptor 4 ligand and contributes to microglial activation. *Cell. Rep.* 2015. **10**: 1626–1638.
- 9 Yip, P. K., Carrillo-Jimenez, A., King, P., Vilalta, A., Nomura, K., Chau, C. C., Egerton, A. M. et al., Galectin-3 released in response to traumatic brain injury acts as an alarmin orchestrating brain immune response and promoting neurodegeneration. *Sci. Rep.* 2017. **7**: 41689.
- 10 Awla, D., Abdulla, A., Regner, S. and Thorlacius, H. TLR4 but not TLR2 regulates inflammation and tissue damage in acute pancreatitis induced by retrograde infusion of taurocholate. *Inflamm. Res.* 2011. **60**: 1093–1098.
- 11 Merza, M., Hartman, H., Rahman, M., Hwaiz, R., Zhang, E., Renstrom, E., Luo, L. et al., Neutrophil extracellular traps induce trypsin activation, inflammation, and tissue damage in mice with severe acute pancreatitis. *Gastroenterology* 2015. **149**: 1920–1931.e1928.
- 12 Fridlender, Z. G., Sun, J., Kim, S., Kapoor, V., Cheng, G., Ling, L., Worthen, G. S. et al., Polarization of tumor-associated neutrophil phenotype by TGF-beta: “N1” versus “N2” TAN. *Cancer Cell* 2009. **16**: 183–194.
- 13 Hsu, D. K., Yang, R. Y., Pan, Z., Yu, L., Salomon, D. R., Fung-Leung, W. P. et al., Targeted disruption of the galectin-3 gene results in attenuated peritoneal inflammatory responses. *Am. J. Pathol.* 2000. **156**: 1073–1083.
- 14 Xue, J., Nguyen, D. T. and Habtezion, A. Aryl hydrocarbon receptor regulates pancreatic IL-22 production and protects mice from acute pancreatitis. *Gastroenterology* 2012. **143**: 1670–1680.
- 15 Cossarizza, A., Chang, H. D., Radbruch, A., Akdis, M., Andra, I., Annunziato, F., Bacher, P. et al., Guidelines for the use of flow cytometry and cell sorting in immunological studies. *Eur. J. Immunol.* 2017. **47**: 1584–1797.
- 16 Volarevic, V., Milovanovic, M., Ljubic, B., Pejnovic, N., Arsenijevic, N., Nilsson, U., Leffler, H. et al., Galectin-3 deficiency prevents concanavalin A-induced hepatitis in mice. *Hepatology* 2012. **55**: 1954–1964.

Abbreviations: AP: acute pancreatitis · BPD: bile-pancreatic duct · FasL: Fas ligand · Gal-3: Galectin-3 · Gal-3^{-/-}: Galectin-3 deficient · MFI: Mean Fluorescence Intensity · WT: wild type

Full correspondence: Prof. Miodrag L. Lukic, MD, PhD; Center for Molecular Medicine and Stem Cell Research, Faculty of Medical Sciences, University of Kragujevac, Svetozara Markovica 69, 34000 Kragujevac, Serbia
E-mail: miodrag.lukic@medf.kg.ac.rs

The peer review history for this article is available at <https://publons.com/publon/10.1002/eji.201847890>

Received: 29/8/2018

Revised: 26/1/2019

Accepted: 18/3/2019

Accepted article online: 20/3/2019